Mine Water Environ (2015) 34:308–319
DOI 10.1007/s10230-015-0326-8

TECHNICAL ARTICLE

Hydrogeochemical and Isotopic Studies of the Kettara Mine Watershed, Morocco

Sana Toughzaoui · Khalid El Amari · Abdelfattah Benkaddour · Mohamed Hibti · Samira Essarraj

Received: 23 November 2013 / Accepted: 30 January 2015 / Published online: 13 February 2015

Abstract Hydrogeological and geochemical studies of the Ketarra abandoned mine watershed showed that the groundwater chemical facies is linked to the drained schist. δ^2H and $\delta^{18}O$ isotope analysis revealed the influence of evaporation. High levels of dissolved ions, including sulphate, in groundwater collected down-gradient of pyrrhotite tailings are evidence of acid mine drainage. However, the groundwater is low in metals and generally complies with Morocco's drinking water standards; only wells down-gradient of the mine waste is not of good quality. Most of the groundwater is acceptable for irrigation and all of it can be used for livestock.

Keywords Groundwater · Acid mine drainage · Sulphide tailings · Lithology

Introduction

The Jebilet massif (Fig. 1) has significant mining potential, particularly in its central part where massive stratiform metal sulphides (mainly iron, copper, and zinc), oriented NNE-SSW, with gossan outcrops, occur along shear corridors (El Harti et al. 2004). This area contains several abandoned mines, including the Kettara Mine, which closed in 1982. Large quantities of pyrrhotite-rich tailings are stockpiled on about 37 ha of fractured schist. These tailings are fine-grained waste from jig processing stored in a tailings pond, and coarse tailings piles dispersed over the rest of the site. They have been evaluated twice as 187,824 m^3, with an error of 2 %, and an inconsistent value of 462,400 m^3 (1.341 million metric tons, t) using the same geophysical methods (Lghoul et al. 2012a, b). However, 2.8 million t of these wastes can be calculated if one considers 8,000,000 t of extracted ore (Bernard et al. 1988) and 65 % weight yield of pyrrhotite concentrate (Ministry of Energy and Mines 1990). Wastes from open pit exploitation of the gossan must also be considered.

The solid wastes are variously coloured, suggesting their reactivity and potential AMD generation. This is confirmed by red, acidic metalliferous solutions (pH 2.8) that occur during rain events (Toughzaoui et al. 2012). The acid and neutralization potentials of these wastes have been estimated at 51–453 kg $CaCO_3$/t and 0–9 kg $CaCO_3$/t, respectively (Hakkou et al. 2008a). The sulphate production rate of the fine tailings was very high (2,000–8,000 SO_4/kg/week) during the first weeks of kinetic testing (Hakkou et al. 2008b); at this average rate, the material should have released more than 161,000 t of sulphate (Lghoul et al. 2012a). However, climatic conditions of the region (mean annual rainfall of 250 mm; annual potential evaporation exceeds 2,500 mm) differ from those under which kinetic tests are performed. Consequently, there is not enough water to produce such quantities of SO_4; tailings permeability is also a limiting parameter. Indeed, in the main dyke, oxidation of the coarse tailings only extends into the upper 75 cm and alteration in the fine-grained tailings pond does not exceed 15 cm beneath the surface, sometimes only 5 cm (Hakkou et al. 2008a). This indicates that for

---

Electronic supplementary material The online version of this article (doi:10.1007/s10230-015-0326-8) contains supplementary material, which is available to authorized users.

S. Toughzaoui · K. E. Amari (✉) · A. Benkaddour · M. Hibti · S. Essarraj
Laboratoire Géoressourses, Unité de Recherche associée au CNRST (URAC 42), Faculté des Sciences et Techniques, Univ Cadi Ayyad, B.P. 549, Bd Abdelkarim Khattabi, 40000 Guéliz, Marrakech, Maroc
e-mail: k.elamari@uca.ma

more than 30 years, AMD production has been limited to a thin layer at the top of the tailings.

The aim of the present work was to highlight the relationship between water chemistry and lithology of the Kettara mine watershed, as well as to use hydrogeologic, geochemical, and isotopic tools to assess the impact of these wastes on groundwater quality. Despite the fact that drinking water is supplied to the population of Kettara village by Morocco's National Office of Drinking Water, the results address concerns about the presence of mine waste in an area where groundwater is the main water source for drinking, irrigation, and livestock.

Geology

The Kettara mine is located in the central part of the Jebilet massif, one of the largest palaeozoic massifs of the Hercynian fold belt of Morocco, extending 170 km EW and 7–40 km NS (Fig. 1b). This massif is considered to be an intracontinental Devonian–Carboniferous rift-basin and consists of three lithotectonic domains, the western, central, and eastern Jebilet, which are separated by major shear zones (Aarab and Beauchamp 1987; Huvelin 1977; Lagarde and Choukroune 1982).

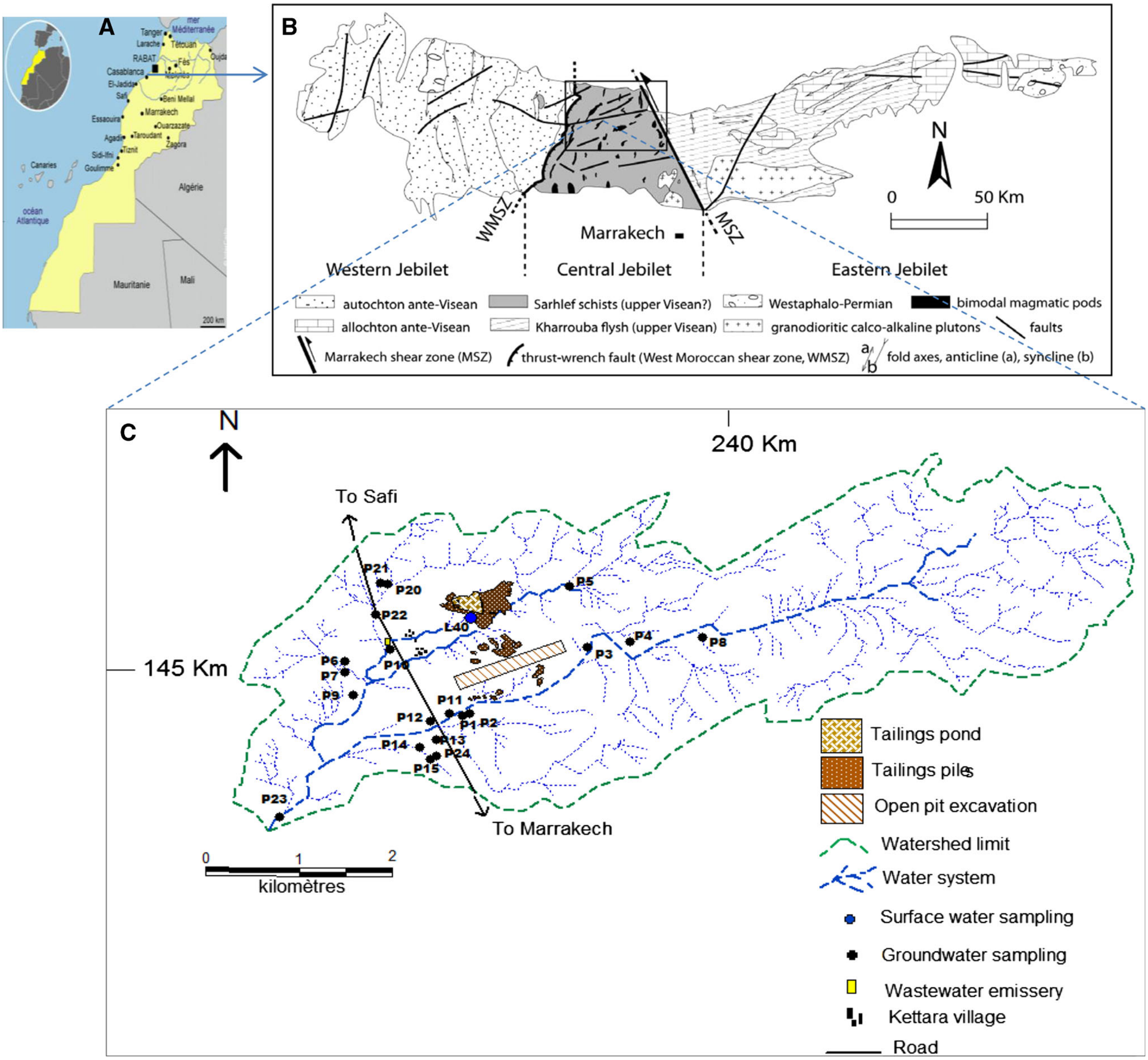

Fig. 1 **a** Location of the Jebilet massif in Morocco; **b** General geologic map of the Jebilet massif (modified from Huvelin 1977); **c** The Kettara watershed and water sampling map: (1) tailings pond, (2) tailing piles, (3) open pit excavation, (4) watershed limit, (5) water system, (6) surface water sampling, (7) groundwater sampling, (8) wastewater emissary, (9) Kettara village, (10) road

The Central Jebilet, where the mine is located, consists of metamorphosed and deformed rocks of Upper Visean-Namurian age with mainly marine sediments (Sarhlef schists) were deposited in an anoxic environment (Beauchamp 1984; Beauchamp et al. 1991). The Sarhlef schists comprise a thick succession of argillites and carbonaceous argillites overlain by carboniferous carbonaceous argillites and limestones. The Central Jebilet unit was deformed during the hercynian orogeny with a major, post-Visean east–west shortening, which led to development of a main regional schistosity S1 (NNE-SSW) and regional folds trending NNE-SSW. This major deformation was associated with a low-grade regional metamorphism, and resulted in a quartz–muscovite–chlorite assemblage. During the Hercynian orogeny, intensive bimodal syntectonic magmatism produced intercalations of lavas and sills and alternating acidic and basic volcanic tuffs.

Sampling and Analytical Methods

To study the hydrogeology and groundwater hydrogeochemistry of the Kettara watershed and to establish the relationship between water the chemistry and lithology, three investigations were undertaken:

- A metallographic study of both ore and gangue and a petrographic study of the host rocks: 11 polished sections were prepared from samples collected from primary dredged spoil and secondary crushed ore, as well as eight thin sections of host rock.
- A structural study to determine the structures that constitute, in such fractured material, the preferred water circulation pathway.
- Hydrogeological and hydrochemical studies to establish piezometric and mineralization maps. Wells in this study are usually excavated in fractured schist, which constitutes the superficial aquifer.

Two sampling campaigns were carried out during a wet season (Feb 03, 2009) and a dry season (May 05, 2009). 24 wells (P1, P2 …) were sampled during each season and one sample of stagnant surface water was collected coming from wastes (L40) during the wet season. This sample was collected near the tailings pond and was considered as the AMD reference in this study. Groundwater sampling points were selected based on their position, up- and down-gradient of tailings.

Temperature, pH, redox potential (Eh), and electrical conductivity (EC) were measured at the sampling site. Chemical analyses focused on cations (Ca^{2+}, Mg^{2+} Na^{+}, K^{+}), anions (Cl^{-}, $SO_4{}^{2-}$, $CO_3{}^{2-}$, $HCO_3{}^{-}$) and metals (Fe, Zn, Cu, Pb, As, Ti, Al, Co, Cd, Cr, Mn, Ni) in the original ore deposit. Isotopic analyses ($\delta^{18}O$ and $\delta^{2}H$) focused on the 15 most representative points (P1, P4, P5, P5′', P7, P9, P10, P11, P12, P14, P20, P21, P23, P24, L40). Chemical analyses were performed by: volumetry, ICP-AES, flame spectrometry, spectroscopy, and laser nephelometry at the Laboratoire Géoressourses of the Earth Science Dept. of the Science and Technics faculty, Marrakech Morocco, and Regional University Center Interface of Fez, Morocco. Isotopic analyses were performed at the National Center of Energy, Sciences and Nuclear Techniques, Rabat, Morocco.

Results and Discussions

Study Area

The Kettara Mine is a part of a small, relatively elongated watershed of approximately 22.7 km^2 (Fig. 1c), with a compact Gravelius index of 1.58. The area is characterized by low density drainage and high branching. Highly fractured schist tends to have very high degrees of permeability. The basin is drained by two main NE-SW oriented wadis (the northern and southern tributaries), which are separated by an elongated hill in the same direction, from which gossan has been excavated. The southern tributary passes south of the mine, and flows along the open gossan pit. The northern tributary is formed by two main branches that join downstream and meet the southern tributary at the basin outlet.

According Haouz Tensift Basin Agency data, the region's climate is continental arid, with low rainfall. Indeed, precipitation in the Jbilet massif is weak and irregular: about 250 mm/year and a high evaporation rate (2,500 mm). Mean annual temperature is 20 °C, with 13.5 °C in winter and 24.5 °C in summer. The flow regime of the wadis in the basin is intermittent and drainage occurs only during rainfall events. There are no perennial streams or rivers in the area (Lghoul et al. 2012a).

Petrography and Metallography

The massive Kettara sulphide deposit is hosted in the Sarlhef schists, which are cleaved and crosscut by basic dykes. Microscopic study of these rocks revealed alternation of meta-siltstones and dominant meta-sandy-siltstone (Fig. 2, photo 1). The host rock mineralogy is dominated by quartz and sericite, often associated with chlorite, locally abundant biotite, and some carbonate minerals (Fig. 2, photo 2). Carbonate layers up to centimeters thick are often observed in the schists.

The ore deposit comprised three types of ores:

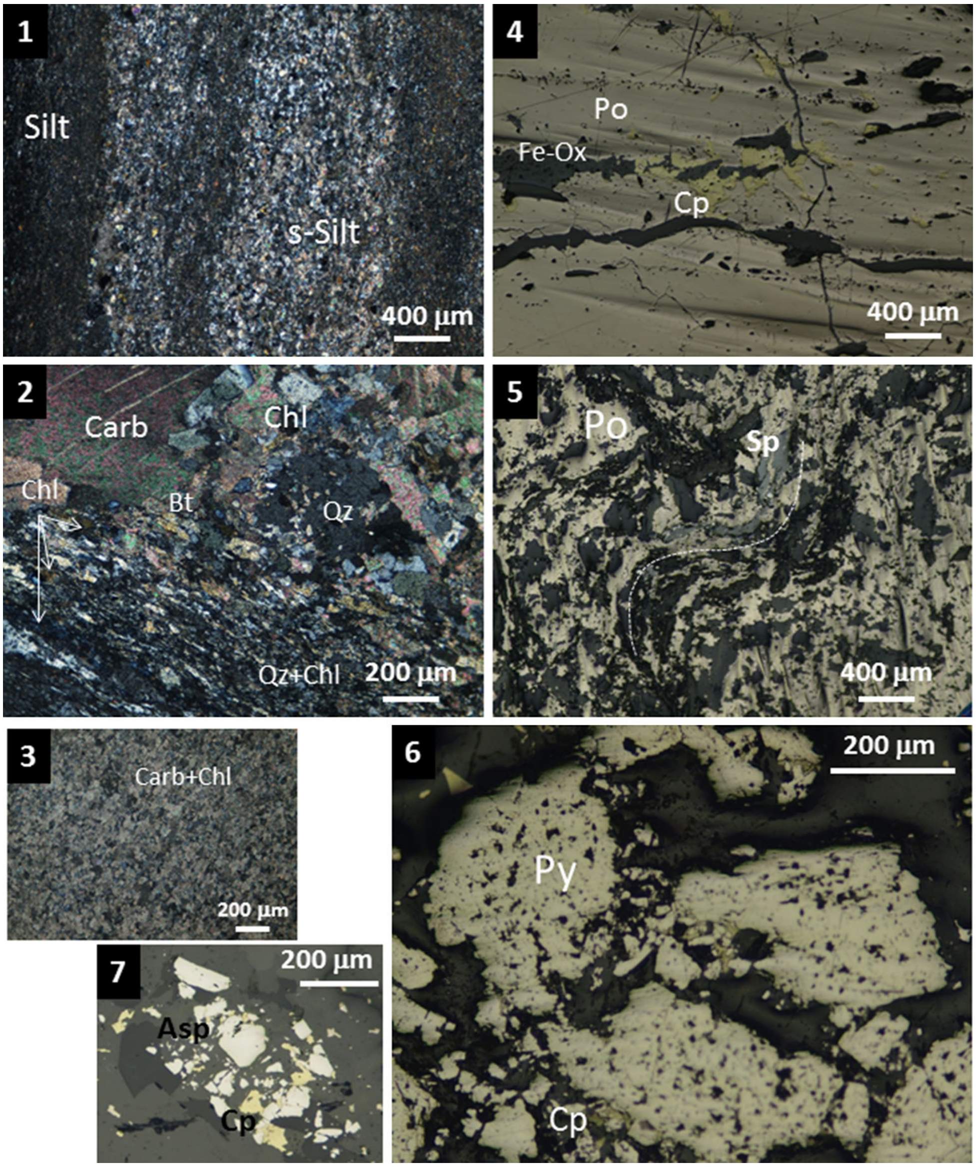

Fig. 2 Photomicrographs showing: (1) Kettara host rocks (meta-sandy-siltstone (s-Silt) dominated by sericites, and meta-siltstones (silt) with quartz-sericites, (2) Host rock mineralogy of Kettara ores: Carb carbonates, Bt: biotite; Chl: chlorite (2 types: brown and blue crystals, Qz : quartz, (3) Local carbonatation of host rocks (Carb) with small scattered chlorite crystals (blue), (4) Massive ore: pyrrhotite (Po), chalcopyrite (Cp) and iron oxides (Fe-ox) resulting of pyrrhotite superficial alteration, (5) Banded and folded ore: pyrrhotite (Po) and sphalerite (Sp), (6) Brecciated ore: pyrite (Py) and later chalcopyrite (Cp), (7) Brecciated ore: arsenopyrite (Asp) and later chalcopyrite (Cp)

- Massive ore: constituted principally of pyrrhotite (80 %) and chalcopyrite (Fig. 2, photo 3) with small amounts of sphalerite. Secondary minerals like iron oxides and hydroxides are observed in some cracks, affecting the ore;
- Banded ore: consisting essentially of alternation of gangue minerals (schist layers and lenses) and massive pyrrhotite, associated with chalcopyrite. This ore contains some fractured pyrite (Fig. 2, photo 4).
- Brecciated ore: dominated by pyrite (Fig. 2, photo 5) and arsenopyrite (glaucodot) (Fig. 2, photo 7). In this type of ore, the later pyrrhotite and chalcopyrite assemblage is less abundant (generally <30 %) than in the massive ore and is often represented only by chalcopyrite. Iron oxides and hydroxides are found locally in this ore type.

The Kettara ores, as well as the host rocks, are affected by strong ductile deformation, which is observed in the hand specimens as well at microscopic scale. This deformation is seen as folding, principally in the massive and banded ore (Fig. 2, photo 4), and by deformation twins seen in the pyrrhotite. Fragile deformation also affected the Kettara ore lens, as observed in the brecciation to cataclastic structure in the brecciated ore. This deformation was observed in ore dominated by pyrite and arsenopyrite (Fig. 2, photos 5 and 6).

Structural Studies

Fracturing studies in the Kettara watershed was focused in the mine waste area to assess the role that fault systems might play in drainage of the AMD (Fig. 3). Structural

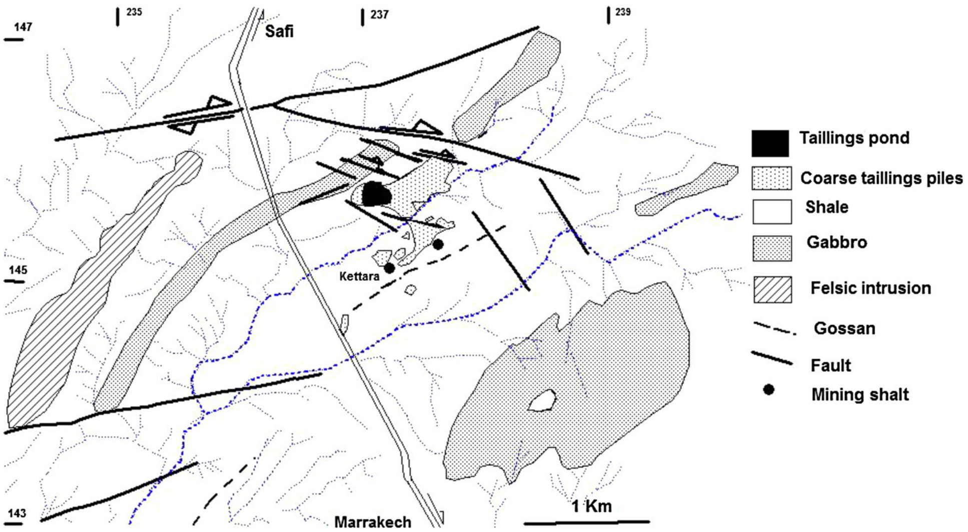

Fig. 3 Simplified structural map of the Kettara mine watershed: (1) tailings pond, (2) coarse tailings piles, (3) shale, (4) gabbro, (5) felsic intrusion, (6) gossan, (7) fault, (8) thalweg, and (9) mine shaft

studies in the Kettara area give evidence of at least two phases of deformation. The major phase, D1, involved very low to low-grade metamorphism, contemporaneous with a post-Visean shortening (the main Hercynian tectonic event in the Moroccan Meseta domain (Michard 1976; Piqué and Michard 1989). This phase is characterized by a well-pronounced, schistose fabric oriented N55 to N70, with a strong dip westward, and a ductile shear zone with the same orientation, often marked by quartz slots in echelon. These structures cannot, in any way, constitute a drain for the water in the areas, as stipulated by Lghoul et al. (2012a), because they have functioned in a ductile regime.

A later phase, D2, is characterized by a S2 crenulation cleavage oriented N130 to N150, sometimes with a very pronounced folding of the S1 cleavage along the N140 faults. In the vicinity of these N140 faults, we note the presence of an open fracture flow post S1. N90–N110 dextral (right lateral) open faults also accompany this late phase. These structures are very well represented in the mine area. Other N140 dextral structures have also been identified, but most are filled by quartz-carbonate. Still, some of the N140 structures, namely those observed at the P2 well, drain large quantities of water. It seems clear that these later structures (N90, N100–110, and N140), at least those that are not locally filled can drain water from the surface into the subsurface.

Hydrogeological Functioning at the Kettara Watershed

Most of the studied sites lie along the wadis. The water flows in a shallow aquifer, which is mainly composed of fractured schists. Piezometric data reveals a general flow from NE to SW (Fig. 4) showing influences of geological structural control. Seasonal effects on the area's groundwater are marked by an average piezometric decline of 0.75 m in the dry season.

Underground water flows along two main axes and converge at the basin outlet, represented by P23 (Fig. 4). The southern tributary feeds wells upstream of the watershed (P3, P4, P8 P5), and those along the southern tributary of the mine (P1, P2, P11, P12, P13, P14, P15, P24), while the northern tributary lies north of the mine, most of which is downstream of the tailings (P6, P7, P9, P10, P20, P21, and P22).

Groundwater Geochemistry in the Kettara Mine Area

Many factors were investigated to determine the major processes that control groundwater chemistry. In general, we focused on the spatial and temporal aspects of the effects of AMD, salinity variations, evolution related to the lithology, and evaporation. Measurements and analyses covered all of the basin and periods of high (February 2009) and low (May 2009) standing water.

AMD Effects

AMD generation is one of the most important problems associated with mining (Gray 1997). Sulphide mineral extraction and processing, especially metal mining, produce milled waste rocks and tailings that are notorious for potential production of AMD, often resulting in pollution of surface water and groundwater (Dold and Fontbote 2001). Indeed, studying the effects of AMD on the watershed helps explain the groundwater hydrochemistry.

Two surface water samples (L40) were collected at the base of the Kettara tailings dam. The tailings were produced by pyrrhotite processing and primarily contain S, Fe, Si,

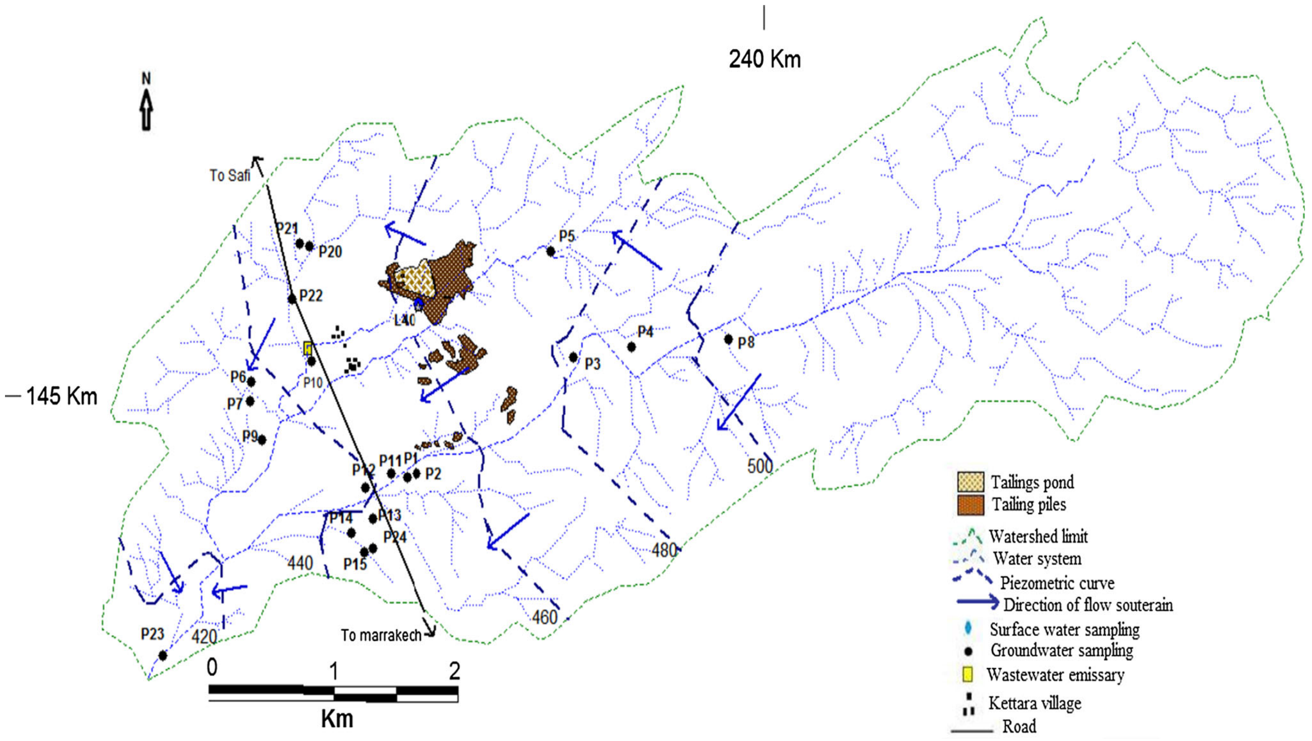

Fig. 4 Piezometric map of Kettara area with sampling points and flow direction (sampling date: Feb., 2009): (1) tailings pond, (2) tailing piles, (3) open pit excavation, (4) watershed limit, (5) water system, (6) piezometric curve, (7) direction of flow souterain (8) surface water, (9) well, (10) wastewater emissary, (11) Kettara village, (12) road

Table 1 Chemical analyses of surface water samples (in mg/L): L40H was collected immediately after a rain event, Feb. 3rd, 2009; L40S: sample collected 2 weeks after a rain event, March 2nd, 2012

	Cl	SO_4	Mg	Ca	K	Na	Al	Co	Cr	Cu	Fe	Mn	Ni	Zn
L40H	71	2,990	324	144	0.2	3	165	1.9	8	17	27	15	0.3	7.0
L40S	532	69,693	31,196	366	0	3	4,893	27	1	240	438	241	4	147

Mg, Ca, K, and Na as major elements, and Cu, Pb, Zn, As, Co, Mn, Ni, Ti, and Cr as trace elements. The water has a pH of 2.8 and an EC of 3340 µS/cm.

It can be seen from Table 1 that there is a great difference in sulfur and metal concentrations over time after a rainfall event. This is explained by the formation, in Kettara's arid climate, of secondary solid sulphate minerals that trap much of the sulfur and metals. Indeed, analyses of several secondary sulphate minerals showed they are rich in these elements (Hakkou et al. 2008a). Formation of AMD and secondary sulphate minerals have been widely studied (Akcil and Koldas 2006; Alpers et al. 1994; Belzile et al. 2004; Collon 2003; Hesketh et al. 2010; Jennings et al. 2008; Lapakko 2002; Nordstrom 1982; Razowska 2001; Rose and Cravotta 1998).

In this study, L40 was considered as the reference of water affected by AMD. It is located upstream of: P6, P7, P9, P10, P20, P21, and P22 (Fig. 5).

In general, groundwater pH is neutral in the upper part of the basin (6.6–7.6) and decreases slightly downstream (6.1–6.8) A table with this data is provided as a supplemental file which accompanies the on-line version of this paper. The lowest pH values were recorded in the immediate vicinity of the tailings. Groundwater sulphate concentrations increase from 56 mg/L for samples collected upstream of the tailings to a concentration of about 2,300 mg/L in well P10. Samples collected downstream of L40 (2,990 mg/L) were most affected by sulphide mineral (pyrrhotite and pyrite are the dominant sulphide minerals at Kettara) reactions:

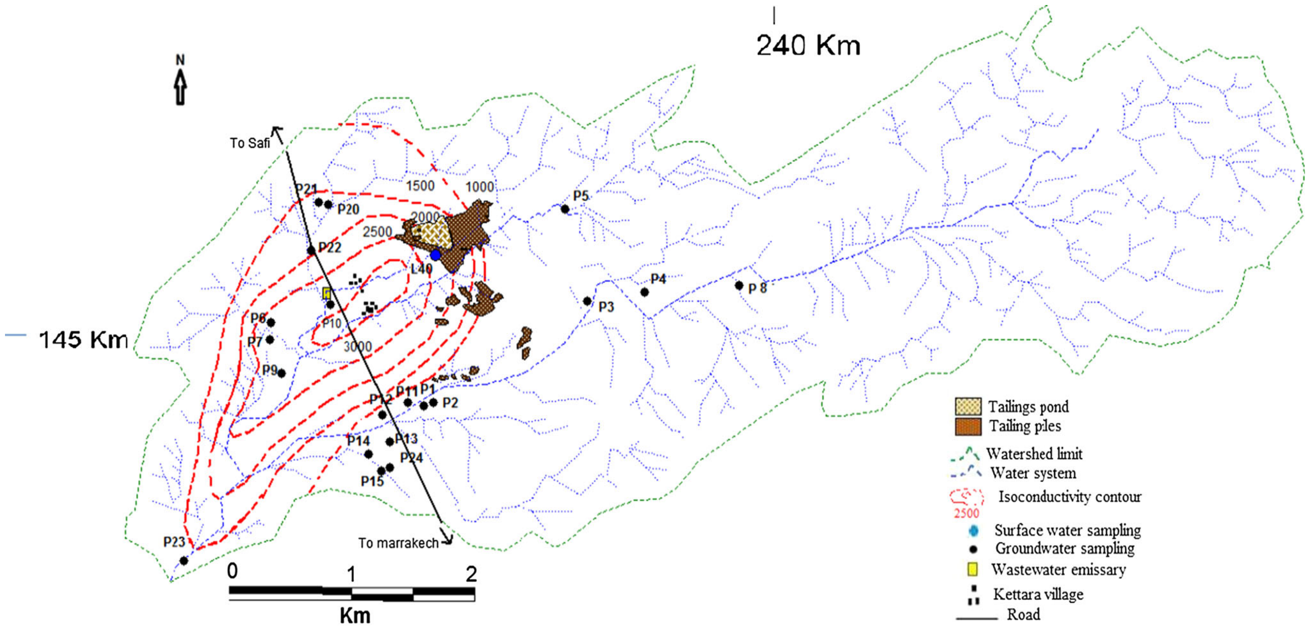

Fig. 5 Evolution of groundwater conductivities (February 2009). (1) Tailings pond, (2) Tailing piles, (3) Open pit excavation, (4) Watershed limit, (5) Water system, (6) Isoconductivity contour, (7) Surface water, (8) Well, (9) Wastewater emissary, (10) Kettara village, (11) road

- Pyrrhotite dissolution:

$$\mathrm{Fe_{1-x}S_{(s)} + [(9-3x)/4]O_{2(aq)} + [(5-3x)/2]\ H_2O \rightarrow (1-x\ )(Fe\ (OH)_{3(s)}) + SO^{2-}_{4(aq)} + 2H^{+}_{(aq)}}$$

- Pyrite oxidation:

$$\mathrm{FeS_2 + \ 7/2\ O_2 + \ H_2O \rightarrow Fe^{2+} + \ 2\ SO_4^{2-} + \ 2H^{+}_{(aq)}}$$

During the wetter weather, in February, the groundwater concentrations of most of the major elements were higher than during the dry weather sampling event in May. For sulphate, the average difference between the two periods is about 105 mg/L. However, the bicarbonate ion concentration was higher in February than in May (mean $_{\text{difference}}$ = 45 mg/L). Chemical analysis of the groundwater collected during the two periods show negligible metal concentrations.

Salinity Variations

Groundwater chemistry is related to the nature and mineralogical composition of the rocks traversed during infiltration, residence time, surface and groundwater circulation, and seasonal meteorological variability, including the amount of rainfall. The hydrochemistry conforms to the structure of the basin. EC recorded during the period of high stands (February 2009) shows three main groups (Fig. 5):

- Water with low EC (650–850 µS/cm) in the upper part of the Kettara basin (P3, P4, P8, and P5) and in wells P1 and P2, which are separated from most of the tailings by a hill.
- Water with moderate EC (850–1,850 µS/cm) in six wells (P11, P12, P13, P14, P15, P24) lying along the southern tributary (Fig. 5). These wells seem to be affected by small piles deposited behind the hill and by some water coming from the northern tributary, which is affected by AMD.
- Water collected in the north-western part of the basin (P20, P21) and immediately downstream of the tailings (P6, P7, P9, and P10) are characterized by higher EC (1,850–3,010 µS/cm). The wells nearest to the tailings show a slight decrease in pH (6.1–6.6). Despite their pH, most of these waters seem to be affected by AMD. The condition of wells P20 and 21 is due to the drainage system faults N110° (Fig. 3).
- At the basin outlet (P23), the water had an intermediate EC (1,387 µS/cm), due to the effect of mixing of water from both tributaries (Fig. 5).

EC showed little temporal variability, with only a slight difference between EC in February 2009 (mean = 1,446 µS/cm) and EC in May of the same year (mean = 1,423 µS/cm). Wells with low conductivities (P1, P2, P3, P4, P8, and P5) differed less (23 µS/cm) than those affected by AMD (P6, P7, P9, and P10, 76 µS/cm).

Evolution Related to Lithology

One of the main challenges was to understand the impact that lithology had on groundwater chemistry. The Kettara

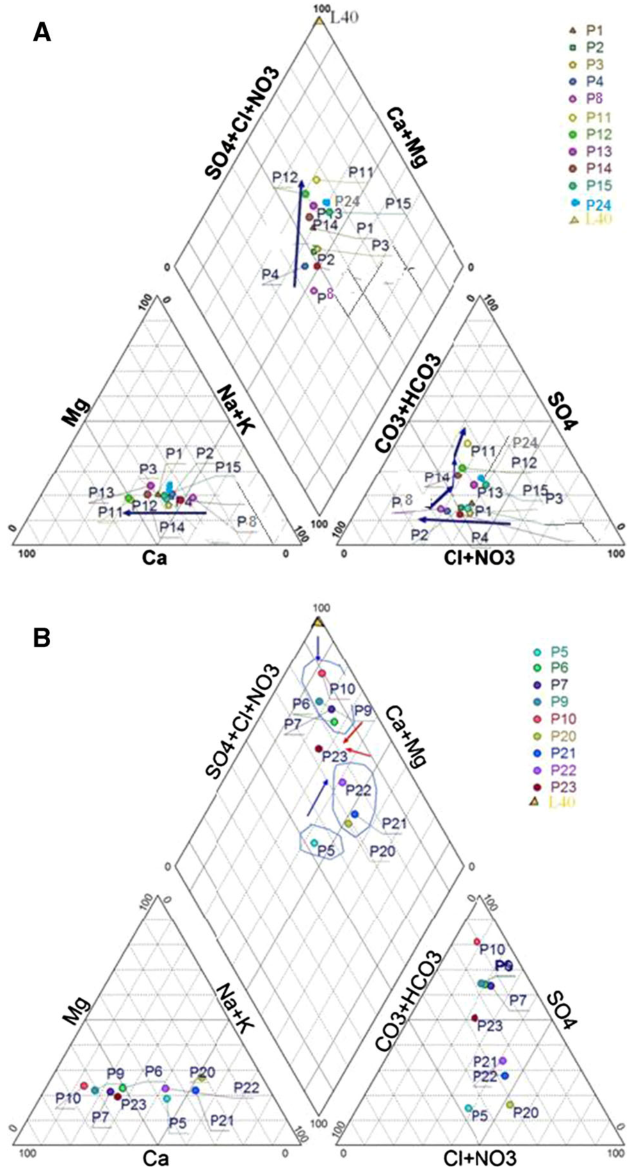

Fig. 6 Piper diagram showing the evolution in water chemistry of Kettara basin

basin is dominated by schists, gabbro outcrops, and felsic intrusions. The effect of lithology on ionic composition is illustrated by a Piper diagram (Fig. 6). Water belongs to three distinct groups that are associated with the geological formations (schists and carbonates):

- The first group (P1, P2, P3, P4, and P5) is rich in Ca–HCO_3–Mg. This facies characterizes the waters of the upper basin, whose chemistry is related to the interaction with magnesium silicate and carbonate minerals.
- The second group include samples collected at P10, P9, P6, P7, P20, and P21, which are downstream of the tailings. These samples are characterized by high dissolved solids with chemical facies dominated by Cl–SO_4–Ca–Mg. This is a result of both AMD and the village wastewater contamination. Water from wells P20 and P21, far from the wastewater emissary, lie on the N110 faults, which conduct water from the tailings area (Fig. 2).
- The third group, from wells along the southern tributary (P11, P12, P13, P14, P15, P24), have an intermediate chemical composition between the two other facies. This is attributed to enrichment in sulphate and chloride originating from waste rock piles associated with open pit exploitation of the gossan. Water chemistry at well P23 illustrates a down-gradient mixing of the two previous groups. Surface water (L40) defines a particular facies, which is hyper-sulphated and is the source of sulphate contamination in the wells down-gradient.

Results projected on binary diagrams (Fig. 7) show that Mg^{2+} and SO_4^{2-} are relatively well correlated (correlation coefficient up to 0.97) with total dissolved ions (TDI), while K^+, HCO_3^-, and Cl^- do not show significant dependence towards TDI.

Increasing Mg content in groundwater is due to weathering of phyllosilicate minerals. In fact, the Kettara

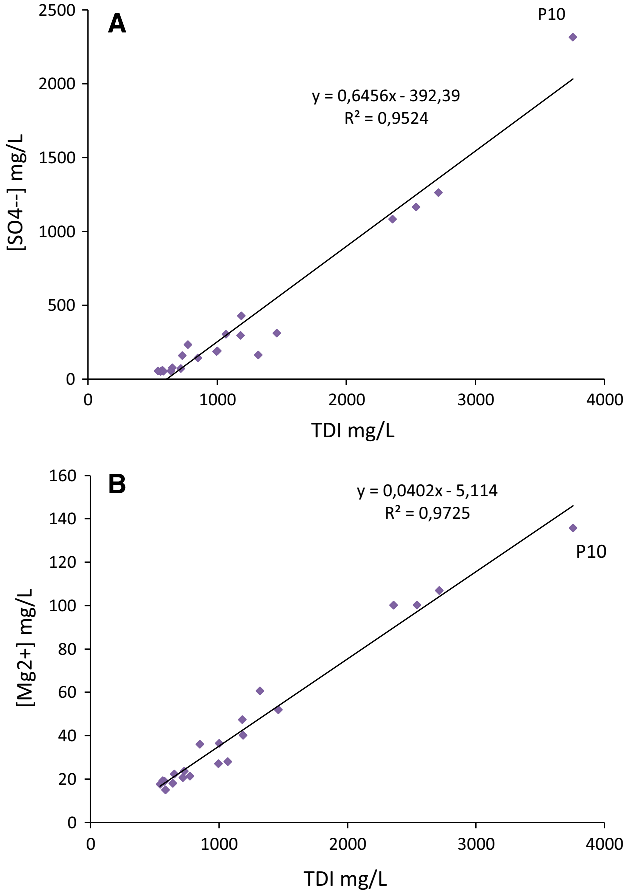

Fig. 7 Sulphate and magnesium concentrations as a function of total dissolved ions in Kettara groundwater

bedrock is rich in phyllosilicates, such as chlorite, biotite, and sericite. Increased acidity in the downstream part of the Kettara basin accelerates this weathering. Dissolved Mg was low (2 mg/L) in the upstream part of the area, while surface water (L40) and groundwater in the vicinity and downstream of the mine (P6, P7, P9, and P10) had the highest Mg concentrations (upto 9 mg/L).

Sulphate ions are the product of sulphide mineral oxidation (mainly pyrrhotite and pyrite). This was confirmed by the high sulphate concentrations in the surface water (L40) in contact with the tailing piles. Despite its short residence time at the surface, sulphate concentrations are very high (upto 2,000 mg/L). The water from wells P6, P7, and P9 are halfway between the two extremes:

- Upstream groundwater characterized by low EC and low sulphate content and
- Groundwater from near the tailing piles (P10), with high EC and high sulphate concentrations.

The mobility of sulphate in aquifers is mainly controlled by precipitation/dissolution of secondary sulphate minerals and redox transformations between sulphate and sulphide coupled with the precipitation/dissolution of metal sulphides. Although sulphate is generally regarded as conservative in groundwater, in soils with abundant iron-oxy-hydroxides and weak competition with other anions, sulphate retention by anion adsorption may occur (Quevauviller et al. 2009).

Hence, SO_4^{2-} is very mobile, which promotes its concentration in the waters of the region, especially down-gradient of the tailings. Indeed, sulphate concentrations were generally much higher than other anions, especially in samples collected down-gradient of the mine.

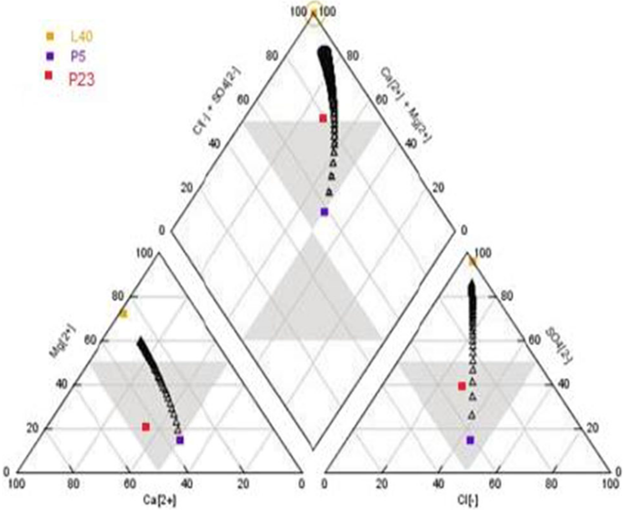

Fig. 8 Piper diagram showing changes in water chemistry according to the model of mixing the water surface (L40) and groundwater (P5)

In order to better understand the factors controlling the water chemistry, a chemical facies simulation of a mixing model was made using the geochemical modelling program, CHESS 2.5. The mixing concerns the two extremes: (a) surface water heavily affected by AMD (L40) and (b) the non-affected waters collected at well P5 at the extreme upstream of the basin (Fig. 8)

In general, the water samples align with the axis of the mixture (Figs. 6, 8). Indeed, the triangular diagram of major anions presents a simple evolution of sulphate and bicarbonate due to mixing between the water in the northern tributary and the better water in the south. Sulphate ions are derived from the infiltration of surface water rich in this element (L40). The diagram of major cations shows an evolving Ca and Mg load, possibly due to exchange reactions. The rainwater washes arable land that is rich in silicate minerals (mica, quartz, etc.), causing infiltration of some cations (Mg^{2+}, Ca^{2+}, etc.).

Evaporation

The $\delta^{18}O$ isotope ratios and $\delta^{2}H$ show the effect of evaporation on aqueous mineralization in the Kettara region. They also allow analysis of the origin and recharge processes (Ndembo Longo 2009; Rozanski et al. 1996), the interaction between surface water and groundwater, and direction of groundwater flow (Xu et al. 2012). The $\delta^{2}H$ and $\delta\ ^{18}O$ contents range between −0.98 and −6.78 ‰ and −41.28 and −15.55 ‰, respectively. Surface water is represented by two samples: L40H collected immediately after a rainfall event and L40S collected 2 weeks after precipitation. The L40S water shows an important evaporation effect, though both $\delta^{2}H$ and $\delta\ ^{18}O$ are enriched. The $\delta^{2}H$ and $\delta\ ^{18}O$ relationships shows that the L40H water sample adheres more closely to the local meteoric line with a ^{2}H excess of about 13 ‰. Some samples show the effect of evaporation along a line with a slope of about 5.4 (Fig. 9).

According to Fig. 9, the water samples fall into four main groups:

- The first group is represented by surface water L40H, which is assumed to be representative of precipitation in the region (Benkaddour et al. 2005).
- The second group mainly includes water from the upstream wells and wells along the southern wadis (P1, P2, P3, P4, P5, P8, P12, P14, and P24). These waters are slightly enriched relative to local meteoric water levels. This enrichment is due to slight amounts of evaporation that occurred before and during infiltration.
- The third group include water samples that are variously distributed on the evaporation line but that all have a degree of evaporation greater than that

Fig. 9 δ ^{18}O/δ ^{2}H relationship for groundwater and surface water from the Kettara watershed area (*MMWL* meteoric water line of the Mediterranean, *LMWL* local meteoric line)

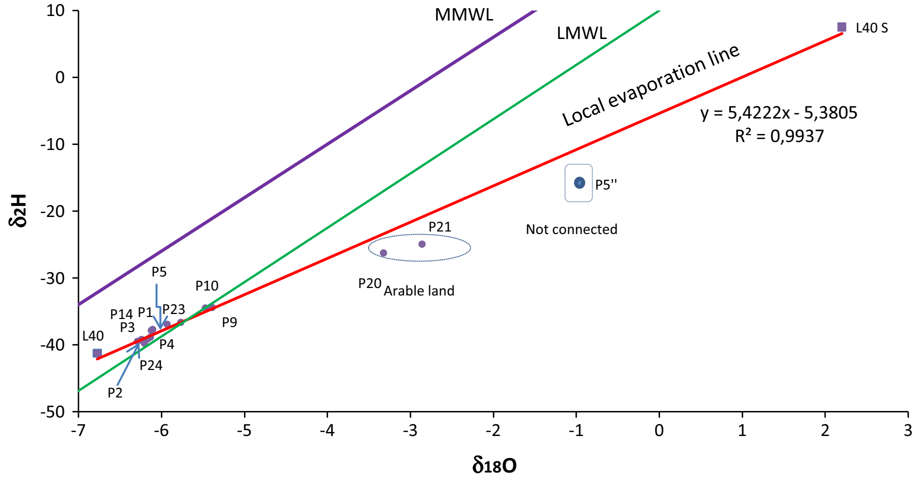

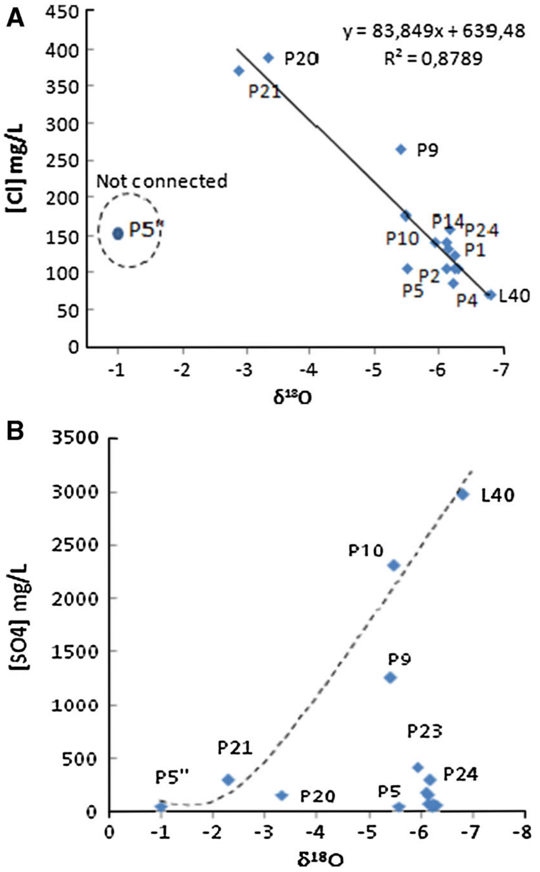

Fig. 10 Relation between δ^{18}O and chlorides and sulphates in the Kettara water basin

observed in group 2: water from wells P20 and P21, which reflect relatively high levels of evaporation, and samples taken from wells P10 and P9 down-gradient of the tailings, which also reflect high levels of evaporation, but are more AMD-influenced. The effects of evaporation in these samples were amplified by the formation of secondary sulphate minerals, which reduced the infiltration rate.

- The fourth group is represented by surface water L40S, which was very strongly affected by evaporation. This is confirmed by the strong isotopic enrichment and very high EC values.

Well P5'' shows a high evaporation effect, even though it is only about 10 m from P5, which has a low evaporation rate, and belongs to group 2. Indeed, P5'' reflects offline water circulation in the area, and is not typical of the mine area.

Enrichment in δ^{18}O is generally accompanied by an increase in Cl^{-} concentrations (Fig. 10). However, for the two NW tailings wells, P20 and P21, the effect of arable soil leaching of aluminosilicates is more pronounced than the phenomenon of evaporation. P5'' is characterized by high level of δ^{18}O and Cl^{-}, this is due to evaporation. The values at P9 may be due to a change in facies that does not affect the nearby well P10.

The relationship between δ^{18}O and sulphate showed that high concentrations of sulphates (L40, P9, P10, and, to a lesser extent, P21) are related to leaching and oxidation of sulphide minerals. These effects are evident at L40. Waters downstream of L40 are rich in sulphate. P10, the groundwater sample with the highest sulphate concentration, could reflect the combined effects of mine tailings and wastewater.

Water Quality in the Kettara Basin

According to the 1986 Moroccan standards for drinking water, the Kettara groundwater is acceptable, with only wells down-gradient of the mine waste (P6, P7, P9, P10, P20, P21, and P22) being not of good quality, due to high EC and elevated concentrations of some elements, including sulphate, chloride, and magnesium (Table 2 and the supplemental table). However, metal concentrations are

Table 2 Moroccan water quality standards (1986) compared with Kettara groundwater; all concentrations in mg/L, electrical conductivity (EC) in µS/cm

	Maximum recommended concentration	Maximum admissible concentration	Minimum required concentration	Water samples meeting the standards
pH	6.5–8.5	9.2	6.0	All samples
EC	1,300	2,700	110	P1, P2, P3, P4, P5, P8, P11, P12, P13, P14, P15, P24
Ca^{2+}	100		10	All samples
Mg^{2+}	100			All except P6, P7, P9, P10
Al	0.05			All samples
SO_4^{2-}	200			All samples except P6, P7, P9, P10, P20, P21, P22, P23
Cl^-	300	750		All samples except P9, P20, P21, P22
Cd	–	0.005	–	All samples
Cr	–	0.05	–	All samples
Cu		1		All samples
Fe	100	0.3		All samples
Mn	20	0.1	–	All samples
Pb	–	0.05	–	All samples
Zn	–	5	–	All samples

low, regardless of the season. This water is suitable for irrigation (Richards 1954), except for water from wells P20 and P21, which should only be used with caution. However, all of these waters comply with the standards for livestock (McKee and Wolf 1963).

Conclusions

Hydrogeological, geochemical, and isotopic studies of the Kettara mine watershed have provided a better understanding of how mine wastes have affected the groundwater, the groundwater's hydrodynamic behaviour, and the relationship of its chemistry to lithology. The superficial aquifer mainly consists of fractured metamorphic (schist-sandstone and schist) facies. The ore is essentially pyrrhotite, pyrite, chalcopyrite, and sphalerite. Groundwater generally flows from the NE to SW and the hydrochemistry of the groundwater up-gradient of the mine waste is linked to the drained schist.

The intermediate chemical composition of the watershed outlet (P23) is due to mixing of groundwater from the northern and southern tributaries. Well water near and downstream of the tailings are rich in sulphate and magnesium associated with the AMD and village sewage. These waters are low in potentially toxic metals initially present in the AMD; these have apparently been removed by the formation of secondary sulphate minerals. Isotopic analyses of $\delta\ ^{2}H$ and $\delta\ ^{18}O$ have revealed the influence of evaporation.

The Kettara watershed groundwater generally complies with Morocco's drinking water standards; only wells downstream of the mine wastes are not of good quality. Most of the groundwater is acceptable for irrigation and all of it can be used for livestock.

Acknowledgments The authors thank the Regional Interface Center of Fes University and the National Center of Energy, Sciences and Nuclear Techniques of Rabat, Morocco, for their contributions of chemical and isotopic analyses.

References

Aarab EL, Beauchamp J (1987) Le magmatisme carbonifère préorogénique des Jebilet centrales (Maroc). Précisions pétrographiques et sédimentaires. Implications géodynamiques. CR Acad Sci II 304:169–175

Akcil A, Koldas S (2006) Acid mine drainage (AMD): causes, treatment and case studies. J Clean Prod 14:1139–1145

Alpers CN, Blowes DW, Nordstrom DK, Jambor JL (1994) Secondary minerals and acid mine-water chemistry. In: Jambor JL, Blowes DW (eds), Environmental geochemistry of sulphide mine-wastes, Short Course-Mineral Assoc Canada, vol 22, pp 247–270

Beauchamp J (1984) Le carbonifère inférieur des Jebilet et de l'Atlas de Marrakech (Maroc): migration et comblement d'un bassin marin. Bull Soc Geol Fr 7-XXVI-6:1025–1032

Beauchamp J, Izart A, Piqué A (1991) Les bassins d'avant-pays de la chaîne hercynienne au Carbonifère inférieur. Can J Earth Sci 28:2024–2041

Belzile N, Yu-Wei Chen, Cai Mei-Fang, Li Yuerong (2004) A review on pyrrhotite oxidation. J Geochem Explor 84:65–76

Benkaddour A, Lamb H, Leng M, Gasse F (2005) Stable isotope records of holocene environmental changes from Moroccan lakes: an imagined synthesis. PAGES 2nd open science meeting. Beijing, China. http://www.pages-igbp.org/download/docs/meeting-products/posters/2005-osm2/Benkaddour-A.pdf

Bernard AJ, Maier OW, Mellal A (1988) Aperçu sur les amas sulfures massif des Hercynides marocaines. Miner Depos 23:104–114

Collon P (2003) Evolution de la qualité de l'eau dans les mines abandonnées du bassin ferrifère lorrain. De l'expérimentation au laboratoire à la modélisation in situ, Thesis

Dold B, Fontbote L (2001) Element cycling and secondary mineralogy in porphyry copper tailings as a function of climate, primary mineralogy, and mineral processing. J Geochem Explor 74:3–55

El Harti A, Banari A, Bachaoui M, Aarab E, El Ghmari A (2004) Etude spectroradiométrique des roches des Jbilet Centrales (Maroc): perspective d'utilisation de la télédétection hyperspecrale pour la cartographie géologique. Télédétection 4(3):251–262

Gray NF (1997) Environmental impact and remediation of acid mine drainage: a management problem. Environ Geol 30(1/2):62–71

Hakkou R, Benzaazoua M, Bussière B (2008a) Acid mine drainage at the abandoned Kettara Mine (Morocco): 1. environmental characterization. Mine Water Environ 27:145–159

Hakkou R, Benzaazoua M, Bussière B (2008b) Acid mine drainage at the abandoned Kettara Mine (Morocco): 2. mine waste geochemical behavior. Mine Water Environ 27:160–170

Hesketh AH, Broadhurst JL, Bryan CG, Van Hille RP, Harrison STL (2010) Biokinetic test for the characterisation of AMD generation potential of sulfide mineral wastes. Hydrometallurgy 104:459–464

Huvelin P (1977) Etude géologique et gitologique du massif hercynien des Jbilet (Maroc occidental). Service Géologique du Maroc No 232 bis:15–18

Jennings SR, Neuman DR, Blicker PS (2008) Acid mine drainage and effects on fish health and ecology: a review. Reclamation Research Group Publ, Bozeman

Lagarde JL, Choukroune P (1982) Cisaillement ductile et granitoïdes syntectoniques: l'exemple du massif hercynien des Jebilet (Maroc). Bull Soc Geol Fr 24:299–307

Lapakko K (2002) Metal mine rock and waste characterization tools: an overview. Report, Mining, mineral and sustainable development, MMSD, IIED, No. 67. http://pubs.iied.org/pdfs/G00559.pdf

Lghoul M, Kchikach A, Hakkou R, Zouhri L, Guerin R, Bendjoudi H, Teíxido T, Penã JA, Enriqué L, Jaffal M, Hanich L (2012a) Etude géophysique et hydrogéologique du site minier abandonné de Kettara (région de Marrakech, Maroc): contribution au projet de réhabilitation. Hydrol Sci J 57(2):370–381

Lghoul M, Teixido T, Pena JA, Hakkou R, Kchikach A, Guérin R, Jaffal M, Zouhri L (2012b) Electrical and seismic tomography used to image the structure of a tailings pond at the abandoned Kettara Mine, Morocco. Mine Water Environ 31:53–61

McKee JE, Wolf HW (eds) (1963) Water quality criteria. California state res central Bd, Publ 3-4, 2nd edn. www.waterboards.ca.gov/publications_forms/publications/general/docs/waterquality_criteria1963.pdf

Michard A (1976) Eléments de Géologie Marocaine. Notes et Mémoires du Service Géologique du Maroc

Ministry of energy and mines (1990) Mine de Kettara. Panorama de l'industrie minière, Royaume du Maroc Ministère de l'énergie et des Mines, Tome 2

Ndembo Longo J (2009) Apport des outils hydrogéochimiques et isotopiques à la gestion de l'aquifère du mont ambakinshasa, république démocratique du Congo. Thesis, Univ d'Avignon, France

Nordstrom DK (1982) Aqueous pyrite oxidation and the consequent formation of secondary iron minerals acid sulphate weathering. Soil Sci Soc Am 10:37–56

Piqué A, Michard A (1989) Moroccan hercynides: a synopsis. The paleozoic sedimentary and tectonic evolution at the northern margin of West Africa. Am J Sci 289:286–330

Quevauviller P, Fouillae AM, Grath J, Ward R (2009) Groundwater monitoring. Water quality measurements series, Publ ISBN 978, Wiley, NY

Razowska L (2001) Changes of groundwater chemistry caused by the flooding of an iron mine (Czestochowa region, southern Poland). J Hydrol 244:17–32

Richards LA (1954) Diagnosis and improvement of saline and alkali soils salinity. US Dept of Agriculture, no. 60, Washington DC. http://www.ars.usda.gov/sp2UserFiles/Place/53102000/hb60_pdf/hb60complete.pdf

Rose AW, Cravotta CA (1998) Geochemistry of coal-mine drainage. In: Brady KBC, Smith MW, Schueck J (eds) Coal mine drainage prediction and pollution prevention in Pennsylvania. Pennsylvania Dept. of Environmental Protection 5600-BK-DEP2256, Harrisburg, pp 1.1–1.22

Rozanski K, Araguas-Araguas L, Gonfiantini R (1996) Isotope patterns of precipitation in the East African region. In: Johnson TC, Odada EO (eds) The Limnology, climatology and paleoclimatology of the East African Lakes. Gordon and Breach Publ, Netherlands, pp 79–94

Toughzaoui S, Benkaddour A, El Amari K, Hibti M, Marah H, Raibi F (2012) Incidence du drainage minier acide sur la qualité des eaux souterraines au niveau de la Mine de Kettara: hydrogéochimies élémentaire et isotopique. Integrated Water Resources Management and Challenges of the Sustainable Development. Proc, IHP-VII Series on Groundwater, UNESCO, Paris, France 4:209–214

Xu X, Werner M, Butzin M, Lohmann G (2012) Water isotope variations in the global ocean model MPI-OM. Center for marine environmental sciences, Univ of Bremen, Germany, Geoscientific Model Development, pp 809–818